International Journal of Science and Research (IJSR)
ISSN (Online): 2319-7064
Index Copernicus Value (2016): 79.57 | Impact Factor (2017): 7.296

High Gain Single Stage Boosting Inverter for Alternative Energy Generation

Ann Maria Paul[1], Aswathi S[2], Nila Thilakan[3], Nimitha Gopinath[4], Dr. Leesha Paul[5]

[1, 2, 3, 4]Pursuing Mtech Power Electronics, NSS College Of Engineering, Palakkad, India

[5]Proffessor, Department of EEE, NSS College Of Engineering, Palakkad, India

Abstract: ***A high gain Single-Stage Boosting Inverter (SSBI) for alternative energy generation is used here. The SSBI has a simple topology and a lower component count as compared to the traditional two stage approach. A tapped inductor is employed to attain high input voltage step-up. SSBI has the advantage of high voltage step-up which can be further increased by adjusting the tapped inductor turns ratio and thus operate off low DC input voltage of a single PV panel. SSBI shares the switches of the power train in a manner that allows merging the DC-DC step up converter stage and the grid tied DC-AC inverter stage. Hence, SSBI is realized in a single stage. Pulse Width Modulation was employed to generate AC voltage output. This method was applied to shape the output voltage. It allowed applying smaller decoupling capacitor value, and low THD output for different types of highly non-linear loads was obtained. Since the efficiency of a solar cell is very low, in order to increase the efficiency, methods are to be undertaken to match the source and load properly. One such method is the Maximum Power Point Tracking (MPPT). Incremental Conductance(IC) method is used to track the maximum power point.***

Keywords: micro-inverter, tapped-inductor, solar PV, MPPT

1. Introduction

A solar micro-inverter, is a device used in photovoltaics that converts direct current (DC) generated by a single solar module to alternating current (AC). The output from several microinverters is combined and often fed to the electrical grid. Microinverters contrast with conventional string and central solar inverters, which are connected to multiple solar modules or panels of the PV system. Each microinverter harvests optimum power by performing maximum power point tracking (MPPT) for its connected module. Simple system design, lower amperage wires, simplified stock management, and added safety are the factors introduced with the microinverter solution. Small inverters rated to handle the output of a single panel are microinverters. Modern grid-tie panels are normally rated between 225 and 275W, so microinverters are typically rated between 190 and 220 W.

Micro inverter topologies for PV power generation are classified into three major groups: the single-stage, the two-stage and the multi-stage types. The multi-stage microinverters are usually comprised of a step-up DC-DC converter front stage, under Maximum Power Point Tracking (MPPT) control, an intermediate high frequency DC-DC converter stage to attain a rectified-sine waveform, and a low frequency inverting stage to interconnect to the grid. The multi-stage power train and the associated high component count results in a costly product. The two-stage micro-inverter can be designed cascading a MPPT controlled step-up DC-DC converter and a grid tied high frequency inverter. While the single-stage topology has to do the voltage step-up, the MPP tracking, and the DC-AC inversion all in one stage.

To convert and connect the solar energy to the grid the low voltage of the PV panel first has to be stepped-up significantly to match the utility level. The traditional boost converter cannot provide the required gain at high efficiency and this poses a challenge to the designer of photovoltaic inverters. Therefore, an extensive research effort is dedicated to developing various topologies of high step up DC-DC converters that can be used in tandem with a half or full bridge inverter to implement a solar power generation system. AC-DC power decoupling problem is another concern typical to single phase DC-AC power systems. A decoupling capacitor on the DC link between the input and output stages is the traditional solution. However, some single stage micro-inverters may require placing the decoupling capacitor at the PV module terminals. It result in a substantial decoupling capacitor value and size.

Single stage topologies that can realize voltage step-up and inversion in a single stage were proposed in the past. In [15], a dual boost inverter was suggested. Here the load is connected differentially between the outputs of two bi-directional boost converters, see Fig. 1. This topology resembles a common H-bridge with the boosting inductors connected to the legs' midpoints. The limited DC step-up gain; circulating currents, which impair the efficiency; and somewhat complicated control are the demerits of this approach. Since the function of C1 and C2 is merely output filtering the decoupling capacitor should be placed at the low voltage input, which is an additional disadvantage. Another single stage solution [16], [17] is shown in Fig. 2. Compared to [15] the topologies in [16], [17] use a single boost inductor; have no circulating currents; have a high voltage DC link and, accordingly, a smaller decoupling capacitor. Also, traditional control methods can be applied.

Moreover, the topologies proposed in [18], [19] may provide other choices for single stage solutions. However, the limited DC step-up of [15]-[19] necessitates using a more expensive high voltage PV panels with 70-100VDC output in order to get the desired dc bus voltage compatible to grid connected inverters. Alternatively, using the popular crystalline silicon modules with the 25-50VDC MPP range, these topologies can implement a two-three panel string inverter, which, as any string architecture, is prone to the mismatch problem.

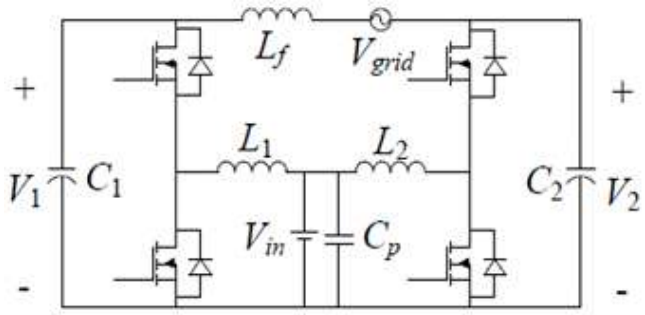

Figure 1: Topology proposed in [15]

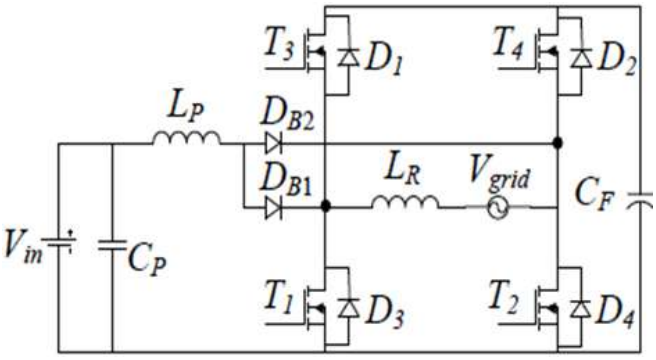

Figure 2: Topology proposed in [17]

2. Single Stage Boosting Inverter (SSBI)

SSBI can achieve higher DC gain and, thus, work off low DC input voltage of a single PV panel. The switches of the power train are shared in such a way that it combines the DC-DC step up converter stage and the grid tied DC-AC inverter stage. Hence, SSBI is comprehended in a single stage. Low value of DC link decoupling capacitor is essential since the power decoupling is done at high voltage. Any control method can be applied here. The proposed schematic diagram of the proposed SSBI is given in Fig 3. SSBI is comprised of semiconductor switches M1..4, arranged in a full bridge configuration; steering diodes D1, D2; DC link diode D3, the tapped inductor W1:W2; the decoupling capacitor Cdc; and the output filter Lo-Co. The resistor R_L represents the load. SSBI is fed by a DC voltage source, Vg, considered to be derived of a single PV panel, and produces utility level AC output voltage Vo. Here, the input current is designated as Ig, the output current is i_o and its average component is Io. The tapped inductor turns ratio, is adjusted in order to obtain a larger voltage step-up and smaller decoupling capacitor, which is placed on high voltage DC bus.

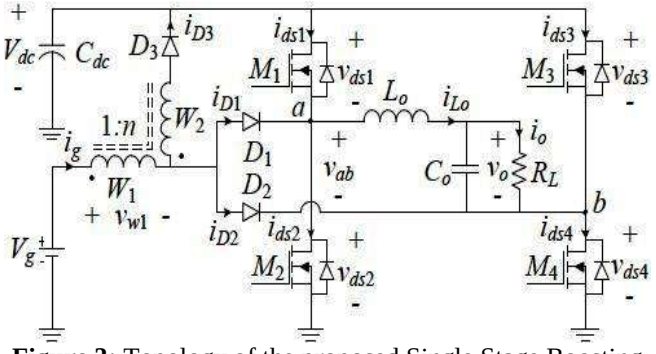

Figure 3: Topology of the proposed Single Stage Boosting Inverter

3. Operating Principle

Principle of operation of the proposed SSBI is hinged on employment of a specialized switching pattern of the H-bridge. Three topological states are formed during the switching cycle in order to create output voltage of positive polarity. Here, buck and boost sub topologies can be identified.

3.1 State A

The switching cycle starts with State A, shown in Fig.4, which persists for a duration of t_a. Here, the switches M1 and M4 are on, whereas switches M2 and M3 are off, D2 conducts and D1, D3 are cut-off. The tapped inductor primary magnetizing inductance Lm is charged from the input voltage source V_g, while the DC voltage V_{dc}, is applied to the input terminals of the output filter so the filter inductance Lo, is charged feeding also the filter capacitor Co, and the load R_L.

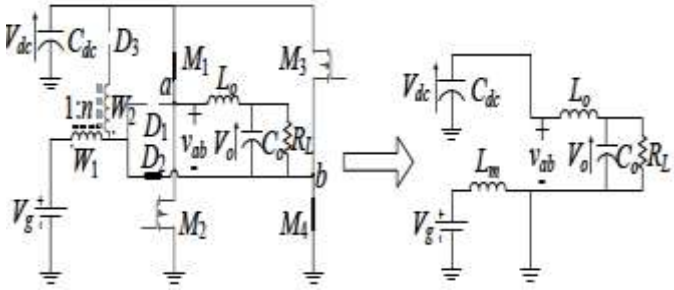

Figure 4: State A operation

3.2 State B

State B, in Fig.5, starts, as the switch M1 is turned off and M2 is turned on, whereas M4 keeps conducting. State B lasts for a duration of t_b. Here, both D1 and D2 conduct while D3 is cut-off. As a result, the tapped inductor magnetizing inductance, Lm, continues charging from the input voltage source Vg, whereas the input terminals of the output filter are shorted so the filter inductance Lo, is discharged to the output capacitor Co and the load R_L .

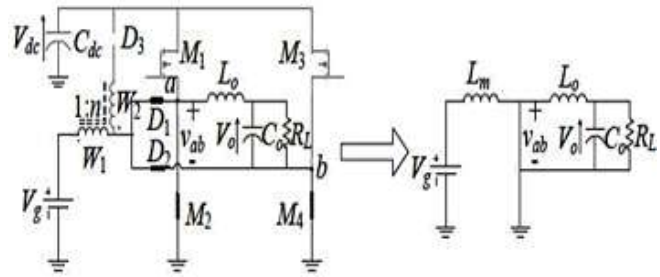

Figure 5: State B operation

3.3 State C

State C, in Fig.6, arises as the switches M1, M3 are turned on and M2, M4 are turned off. State C lasts for duration of tc, and completes the switching cycle. Here, both D1, D2 are cut-off and D3 conducts; Lm, is discharged via both windings and D3 into the DC link capacitor, Cdc, while the input terminals of the output filter are shorted and the filter inductance Lo, feeds the output capacitor Co, and the load RL.

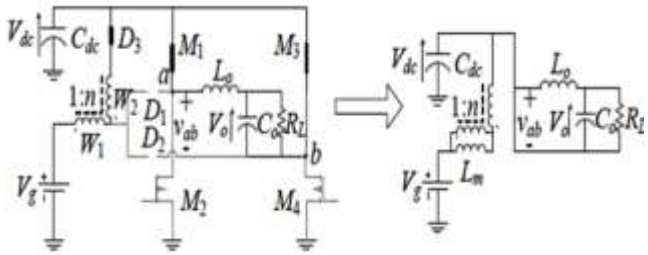

Figure 6: State C operation

Complementary switching states A, B, C are formed by the controller in order to generate output voltage of negative polarity. Proper switching signals for the H-bridge switches should be created of the given buck and boost switching functions and the output polarity signal Sbk(Dbk), Sbst(Dbst), P, respectively. S1..S4 represents the driving signals of the switches M1…M4 respectively. The required Boolean functions can be derived as:

$$S_1 = \overline{\overline{P \cdot S_{bk}} \cdot S_{bst}}$$
$$S_2 = \overline{P \cdot S_{bk}} \cdot S_{bst}$$
$$S_3 = \overline{\overline{P} \cdot S_{bk}} \cdot S_{bst}$$
$$S_4 = \overline{\overline{P} \cdot S_{bk}} \cdot S_{bst}$$

There are 3! possible permutations or state sequences since the switching cycle of SSBI is involved of three states. In other words, the order of appearance of the states is not unique and other possibilities exist, i. e. A-C-B, C-B-A etc. An ideal SSBI can produce same DC-DC conversion ratio under any of these switching regimes. However, some state sequences may require switches to be activated twice per switching cycle, which is unwanted in practice due to increased switching loss and/or extremely narrow on time.

4. SSBI Analysis

To ease the analysis approach the following assumptions are adopted: (a) all semiconductors are ideal with zero on resistance and voltage drop; (b) the decoupling capacitor and the output filter capacitor are sufficiently large and their voltage ripple is negligible; (c) continuous current operation of both the tapped inductor and the output filter inductor is assumed.

4.1 Derivation of Voltage Conversion Ratio

The converter's equivalent circuit discloses that the power stage operates as a boost-derived tapped inductor DC-DC converter merged with a buck-derived full-bridge DC-AC inverter. t_a, t_b and t_c are the extent of states A, B and C respectively and T_s=t_a,+ t_b+t_c is the switching period. The time interval devoted to charging the primary winding of the tapped inductor, that is boost charging state takes place during the states A and B, whereas, boost discharge takes place in state C. The total duration of the boost charging is, therefore:

$$t_{bst}=t_a+t_b$$

Accordingly, the resulting boost duty cycle, D_{bst} is

$$D_{bst}=\frac{t_a+t_b}{T_s}$$

Hence, SSBI performs the DC-DC step-up conversion function identically to the tapped inductor boost converter. The DC-DC voltage conversion ratio of SSBI is

$$M_{bst}=\frac{V_{dc}}{V_g}=\frac{1+nD_{bst}}{1-D_{bst}}$$

The time interval devoted to charging the output inductor, Lo, that is the buck charging state, occurs in state A, whereas buck discharge takes place in states B and C while the terminals of the output filter are shorted. Thus, the time duration of the buck charging is:

$$t_{bk}=t_a$$

Accordingly, the resulting buck duty cycle, Dbk, is

$$D_{bk}=\frac{t_a}{T_s}$$

Clearly, under CCM condition of the output filter inductor, the voltage gain of the output section is identical to that of a buck converter and is given by:

$$M_{bst}=\frac{V_o}{V_{dc}}=D_{bk}$$

Hence, the overall DC-AC voltage conversion ratio, M can be derived as followed:

$$M_{bst}=\frac{V_o}{V_g}=\frac{(1+nD_{bst})D_{bk}}{1-D_{bst}}$$

In stand-alone application in order to achieve a sinusoidal output voltage Vo of requiredl amplitude and frequency, the buck duty ratio, Dbk is modulated. Whereas the boost duty ratio, Dbst, is adjusted to fulfill load power demand and so stabilize the DC link voltage, Vdc. It should be noted that buck duty ratio, Dbk, should be smaller than the boost duty ratio, Dbst, at all times: Dbk < Dbst.

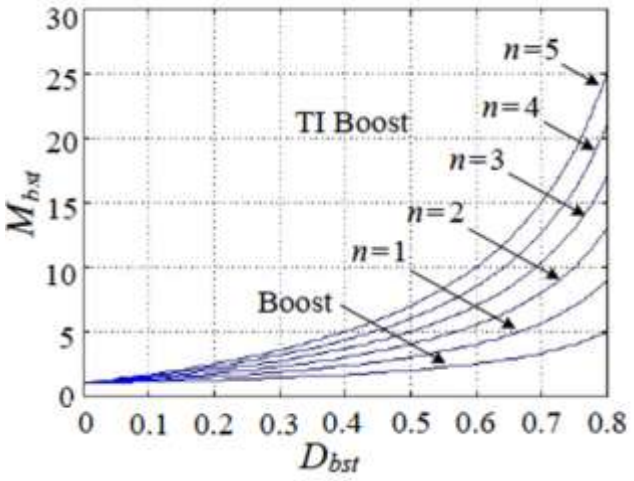

Figure 7: Comparison of conversion ratio, Mbst, of the traditional boost and the tapped inductor (TI) boost converters

5. Maximum Power Point Tracking (MPPT)

The efficiency of a solar cell is very low. In order to increase the efficiency, methods are to be undertaken to match the source and load properly. One such method is the Maximum Power Point Tracking. This is a technique used to obtain the maximum possible power from a varying source. In photo-

voltaic systems the I-V curve is non-linear, thereby making it hard to be used to power a certain load. This is done by utilizing a boost converter whose duty cycle is varied by using a MPPT algorithm.

Incremental Conductance method uses the PV array's incremental conductance to calculate the sign of dI/dV. When it is equal and opposite to the value of I/V (where dI/dV= 0) the algorithm learns that the maximum power point is achieved and thus it stops and gives the corresponding value of operating voltage for MPP. This method tracks rapidly changing irradiation conditions more accurately than PO method.This algorithm uses incremental measurements on the change in conductance of the photovoltaic array. By comparing these calculated incremental measurements, we can calculate whether there was an increase or decrease in power since it was last measured. The incremental conductance is defined dI/dV as By comparing this measurement to the actual conductance of the photovoltaic array, one can determine which side of the MPP the current operating point is located. The disadvantage of the perturb and observe method cannot track the peak power under fast varying atmospheric condition. This is overcomed by IC method.

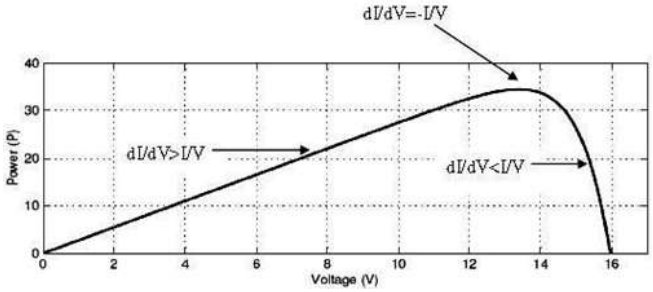

Figure 8: PV panel power curve

The IC can determine that the MPPT has reached the MPP and stop perturbing the operating point. If this condition is not met, the direction in which the MPPT operating point must be perturbed can be calculated using the relationship between dl/dV and I/V.This relationship is derived from the fact that dP/dV is negative when the MPPT is to the right of the MPP and positive when it is to the left of the MPP.Figure above shows that the slope of the P-V array power curve is zero at The MPP, increasing on the left of the MPP and decreasing on the Right hand side of the MPP.

One disadvantage of this is the increased complexity when compared with PO. This algorithm has fewer branches for each node and is less complicated than the PO algorithms flowchart; however, the simplicity of the algorithm flowchart does not account for the increased complexity of binary calculations required for this algorithm.Since calculation of both the InC and conductance requires the use of division, a large amount of processing power is necessary in order to acquire the result before the next sample time.

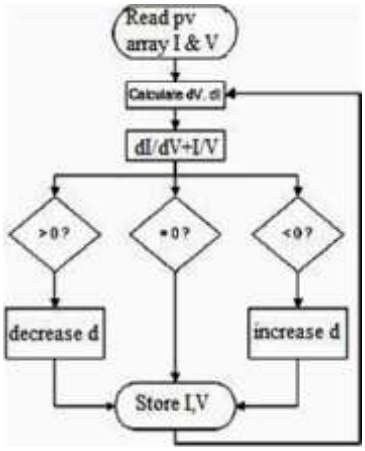

Figure 9: IC flowchart

6. Simulation and Test Result

A stand-alone variant of the proposed SSBI and its control circuits were implemented using Simulink. Simulation waveforms support the theoretical predictions. Under the PWM control the proposed SSBI can deliver high DC input voltage step-up as well as high quality AC output. Due to the superior transient response of the controller, the substantial ripple component of the DC link voltage has no negative effect on the quality of the AC output. Lower decoupling capacitor can be employed without compromising DC-AC decoupling. The controller required no sensing of the AC output voltage is an advantage of this approach. Hence, there is no need for isolated floating sensors, which further simplifies the circuitry suitable for distribution.

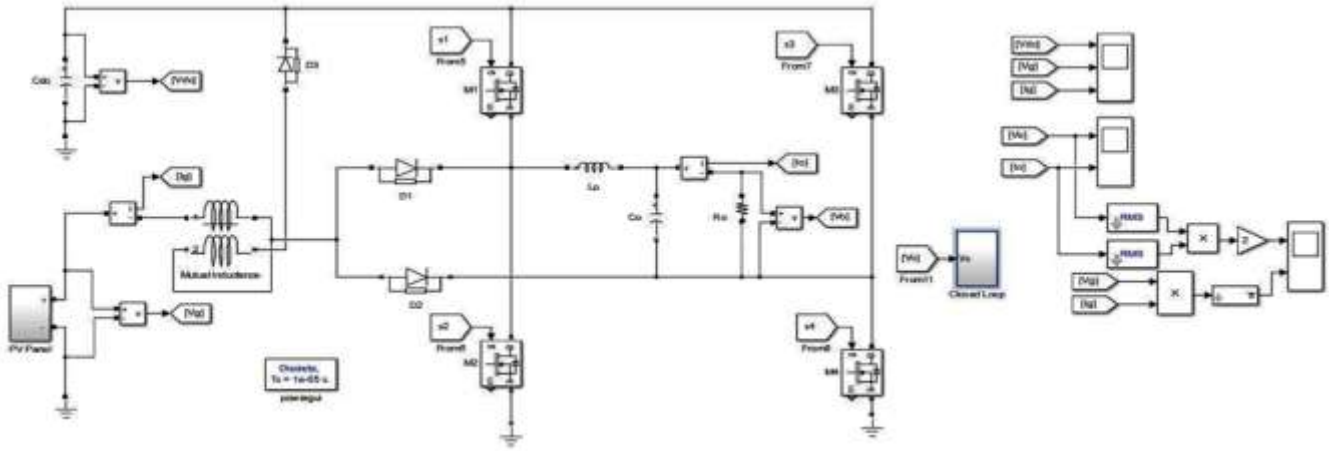

Figure 10: Simulink model of SSBI with R load

The PV array can be simulated with an equivalent circuit model based on the PV model. PV modules are connected in series or in parallel in order to model the PV array block that accepts irradiation in W/m^2 and temperature in degree centigrade and provides array current and voltage that can be measured using current measurement and voltage measurement block respectively. Input to the MPPT block is photovoltaic current and photovoltaic voltage and the output is duty cycle. PWM wave for converter switch is generated from the duty cycle obtained by MPPT. A SSBI is supplied by a 48V solar panel. When a 48V PV Panel is supplied to a SSBI we get an output voltage of 110V. A good quality of AC output waveform is obtained.

Fig. below shows the waveforms of input and output voltage, along with the output inductor current. The measurements were taken at three different power levels at constant input voltage. SSBI generated high quality AC output voltage in a wide range of output power.

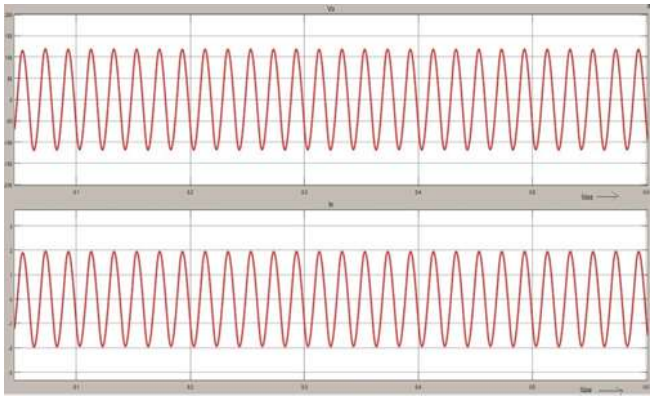

Figure 11: Waveform showing AC output voltage

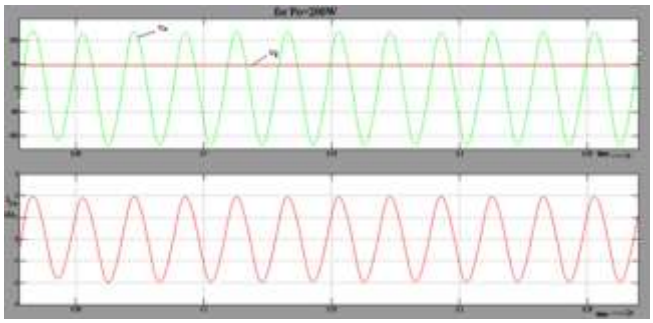

Figure 12: Waveform for 200KW

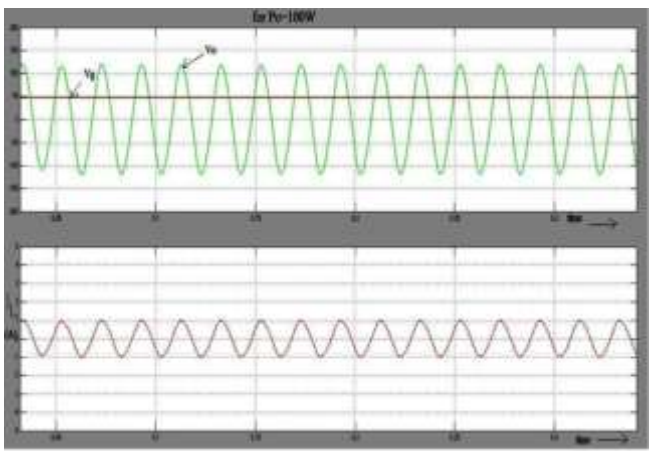

Figure 13: Waveform for 100KW

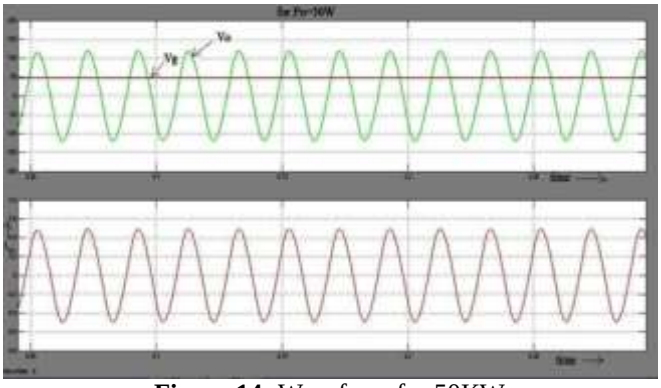

Figure 14: Waveform for 50KW

Table 1: Comparison of Single Stage and Two Stage Topologies

Class	Topology	Sw	D	Vin [V]	Pout [W]	max. Eff. [%]
Single-stage	SSBI	4	3	35-48	200	89.3
	[5]	4	2	48	500	80
	[6]	4	2	90	300	87
	[7]	6	0	30	50	87
	[8]	5	3	92	170	87
Two-stage	[9]	7	3	22-40	250	92
	[10]	6	2	31-51	210	98.2
	[11]	8	2	38-50	2000	93.9
	[12]	8	4	20	250	92.5

Several different load types were presented to SSBI. The measured THD of the output voltage was 5.56%, 9.78%, respectively for linear RL load and non linear load.

Peak efficiency of 89.3% was achieved by a SSBI topology. The conduction losses of the steering diodes, D1 and D2 were identified as the major reason of efficiency drop at relatively low input voltage level. However, since it is a rather common practice to install a blocking diode in series with a PV panel to prevent back flow, such configuration and the associated losses are comparable to some other approaches. Comparison of the proposed SSBI with selected single and two-stage topologies is presented in Table below. SSBI has the best efficiency performance among the single stage topologies. Another conclusion arises when these two classes are compared. Obviously, it is a choice of performance vs. cost: two-stage inverters attain better efficiency; however, at the expenditure of using about twice the number of active switches than the single-stage topologies.

In particular, SSBI is compared with a full bridge based two-stage topology. The former has a total of 4 switches and 3 diodes, whereas the latter used 8 switches and 4 diodes yet, the reported efficiency was 89.3% and 92.5% respectively.

7. Conclusion

A high gain single-stage boosting inverter for alternative energy generation applications is simulated. A tapped inductor is employed to attain high input voltage step-up and so

allows operation from low DC input voltage. The proposed SSBI topology has the advantage of high voltage step-up which can be further improved by adjusting the tapped inductor turns ratio. By adjusting the boost duty cycle Dbst the SSBI can control the dc link voltage, whereas by varying the buck duty cycle, Dbk, the output waveform can be shaped. The AC-DC power decoupling is attained on the high voltage DC link and therefore requires a relatively low capacitance value. PWM control method was applied to shape the output voltage. It allowed applying yet smaller decoupling capacitor value, and low THD output for different types of highly non-linear loads was obtained. A peak efficiency of 89.3% was achieved.

8. Acknowledgment

We would like to thank our guide and parents who has helped us in all possible ways towards the successful completion of this work.

References

[1] Alexander Abramovitz.Ben Zhao.Keyue Smedley."High-Gain Single-Stage BoostingnInverter for Photovoltaic Applications" IEEE Trans. Power Electron., vol. 31,issue5,no. 11, pp. 15677476,May 2016.
[2] H. Patel and V. Agarwal, A single-stage single-phase transformer-less doubly grounded grid-connected PV interface, IEEE Trans. Energy Convers., vol. 24, no.1, pp. 93101, Mar. 2009.
[3] B. Yang, Y. Zhao, and X. He, Design and analysis of a grid-connected photovoltaic power system, IEEE Trans. Power Electron., vol. 25, no. 4, pp. 9921000, Apr. 2010.
[4] C. Pan, C. Lai, and M. Cheng, A novel integrated single-phase inverter with auxiliary step-up circuit for low-voltage alternative energy source applications, IEEE Trans. Power Electron., vol. 25, no. 9, pp. 22342241, Sep. 2010.
[5] N. Kasa, H. Ogawa, T. Iida, and H. Iwamoto, A transformer-less inverter using buck-boost type chopper circuit for photovoltaic power system, in Proc. IEEE Int. Conf. Power Electron. Drive Syst., 1999, pp. 653658.
[6] S. Jain and V. Agarwal, A single-stage grid connected inverter topology for solar PV systems with maximum power point tracking, IEEE Trans.Power Electron., vol. 22, no. 5, pp. 19281940, Sep. 2007., ISSN : 2248-9622, Vol. 3, Issue 6, Nov-Dec 2013, pp.667-674
[7] M. Kusakawa, H. Nagayoshi, K. Kamisako, and K. Kurokawa, Further improvement of a transformerless, voltage-boosting inverter for AC modules, Solar Energy Mater. Solar Cells, vol. 67, no. 14, pp. 379387, Mar. 2001.
[8] C. Yang, Y. Chang, C. Li, et al, A module-integrated isolated solar micro-inverter, in Proc. IEEE Int. Conf. Ind. Info., 2012, pp. 780785..
[9] D. Cao, S. Jiang, F. Z. Peng, and Y. Li, Low cost transformer isolated boost halfbridge micro-inverter for single-phase grid-connected photovoltaic system, in Proc. IEEE Appl. Power Electron. Conf., 2012, pp. 7178.
[10] Soeren Baekhoej Kjaer, John K. Pedersen, Frede Blaabjerg,"A Review of Single-Phase Grid-Connected Inverters for Photovoltaic Modules"IEEE transactions on industry applications, vol. 41, no. 5, september/october 2005.
[11] Quan Li,Peter Wolfs."A Current Fed Two-Inductor Boost ConverterWith an Integrated Magnetic Structure and Passive Lossless Snubbers for Photovoltaic Module Integrated Converter Applications" IEEE transactions on power electronics, vol. 22, no. 1, january 2007.
[12] Chaitanya Vartak, Alexander Abramovitz Keuye Smedley"Analysis and Design of Energy Regenerative Snubber for Transformer Isolated Converters"IEEE Transactions on Power Electronics
[13] Haibing Hu, Souhib Harb, Nasser Kutkut, Issa Batarseh, and Z. John Shen."A Review of Power Decoupling Techniques for Microinverters With Three Different Decoupling Capacitor Locations in PV Systems" IEEE transactions on power electronics, vol. 28, no. 6, JUNE 2013.
[14] R. O. Caceres and I. Barbi, A boost DC-AC converter: analysis, design, and experimentation, IEEE Trans. Power Electron., vol. 14, no. 1, pp. 134141, Jan. 1999.
[15] [15] H. Ribeiro, F. Silva, S. Pinto and B. Borges, Single stage inverter for PV applications with one cycle sampling technique in the MPPT algorithm, in Proc. 35th Annu. Conf. IEEE Ind. Electron., 2009, pp. 842849.
[16] H. Ribeiro, A. Pinto and B. Borges, Single-stage DC-AC converter for photovoltaic systems, in Proc. IEEE Energy Convers. Congr. Expo., 2010, pp. 604610.
[17] T. Liang, J. Shyu, and J. Chen, A novel DC/AC boost inverter, in Proc. IEEE Energy Convers. Eng. Conf., 2002, pp. 629634.
[18] K. M. Smedley, S. Cuk, One-cycle control of switching converters, IEEE Trans. Power Electron., vol. 10, no. 6, pp. 625633, Nov. 1995.